Design and Performance of the H_∞ Controller for the Beam-Waveguide Antennas

Wodek Gawronski*

ABSTRACT. — The linear-quadratic-Gaussian (LQG) controllers are currently implemented at the beam-waveguide (BWG) antennas. Each BWG antenna has a different set of LQG coefficients, obtained by tuning and testing each controller individually. Individual coefficients for each antenna are necessary, since the antenna dynamics are not identical and the derivation of the LQG coefficients is a labor-intensive process. Hence, the process could be simplified by using single set of coefficients for all BWG antennas. The purpose of the work reported here is to develop a single set of servo coefficients for all BWG antennas. This is achieved by using the H_∞ controller approach and a robust design technique. In this article, the analysis of the H_∞ controller was performed, and the results obtained (by executing over 10,000 Monte Carlo simulations) showed that it is feasible to use a single set of the H_∞ controller coefficients at all BWG antennas, and that the H_∞ controller performance is similar to or exceeds the "standard" LQG controller performance, i.e., except for the DSS-25 antenna controller performance. Note that the latter controller was derived exceptionally strong. At the remaining antennas, the controller coefficients are weaker, and they represent the "standard" LQG performance. This approach simplifies the development of the controller coefficients for BWG antennas, and simplifies the servo performance evaluation, since the performance should be similar for all six BWG antennas.

I. Introduction

In order to achieve precise pointing, the linear-quadratic-Gaussian (LQG) controllers are implemented at the Deep Space Network (DSN) antennas. LQG controllers are model-based controllers, i.e., the control algorithm includes the antenna model. The model consists of equations describing the open-loop antenna dynamics. The antenna model in the controller algorithm estimates antenna dynamics, in order to suppress antenna vibrations. If the model estimate mismatches the actual dynamics, the controller (and antenna) becomes unstable.

The model (antenna dynamics equations) for each of the beam-waveguide (BWG) antennas is derived from the field data, using the system identification procedure. Thus, for each axis, six models of the BWG antennas — DSS-24, DSS-25, DSS-26, DSS-34, DSS-54, and DSS-55 —

* Communications Ground Systems Section.

The research described in this publication was carried out by the Jet Propulsion Laboratory, California Institute of Technology, under a contract with the National Aeronautics and Space Administration.

need to be derived. They are not identical; therefore, LQG controllers are derived individually for each antenna. In this project, a single model of antenna is used for all six antennas, which leads to a single set of servo coefficients for all BWG antennas.

The LQG coefficients shall be derived for each antenna separately, and the derivation is a labor-intensive process, composed of 10 steps.[1] The purpose of this article is to derive a single servo-coefficient set for all BWG antennas, to achieve similar or better performance than the current LQG controllers. This is achieved by using the H_∞ controller and robust design technique. The H_∞ control of antennas and telescopes has been deliberated for some time [1–4], but never actually implemented. The robust approach in the antenna controller design has not been yet considered.

The combination of the H_∞ control and robust design consists of four steps:

(1) Deriving an uncertain model that spans properties of all six antennas.

(2) Develop an H_∞ controller that is stable with the uncertain model.

(3) Run Monte Carlo simulations to verify the performance of the controller.

(4) Verify the H_∞ controller performance with all six antennas.

II. Description of the BWG Antenna Models

The antenna model, as presented here, is a set of equations that describes the dynamics of the rate-loop system (i.e., antenna hardware). There are two independent models for each antenna — one describes the dynamics in the azimuth axis, another one in the elevation axis. In this article, only the azimuth models of the BWG antennas are analyzed. The description includes the model equations, magnitudes of the transfer functions, and parameters for each antenna model (modal damping and frequencies and their variations).

An antenna model is a set of the following difference (state-space) equations:

$$\begin{aligned} x(i+1) &= Ax(i) + Bu(i) \\ y(i) &= Cx(i) \end{aligned} \tag{1}$$

where x is the state vector $(\mathrm{n}\times 1)$, u is the rate command (deg/s), y is the antenna position (deg), A is the state matrix, $(\mathrm{n}\times\mathrm{n})$, B is the input matrix $(\mathrm{n}\times 1)$, and C is the output matrix $(1\times\mathrm{n})$, and n is the dimension of the model (for BWG antennas, $n \le 10$). The state vector x describes antenna dynamics, and its physical meaning depends on the selection of coordinates. Thus, (A,B,C) parameters characterize the antenna dynamics.

The system identification is a method that allows one to determine the (A,B,C) parameters from the antenna measured input and output data; see for example [5,6]. Hence, one obtains matrices A, B, and C from the field data, which is the accurate way to capture antenna dynamics.

---

[1] W. Gawronski, *Design Process for DSN Antenna Servo Controller Coefficients*, document number 893-000045-2 (internal document), Jet Propulsion Laboratory, Pasadena, California, September 25, 2007.

The rate-loop transfer function is the analytical description of the antenna response (encoder measurements) caused by the antenna sinusoidal rate input, at different frequencies. This characterization of the dynamics describes the rate-loop properties over the entire spectrum of frequencies within the bandwidth of interest.

The following antennas are considered: DSS-24, DSS-25, DSS-26, DSS-34, DSS-54, and DSS-55. The magnitudes of the rate-loop transfer functions of the six antenna models are shown in Figure 1. The figure shows three modes of vibration (or resonances) in the model. The first two resonances are the most pronounced, while the third one is below the noise level; thus, it is considered insignificant in the development of the uncertain model. The first two resonances differ in frequency, and in resonant amplitudes (the latter depend on modal damping). Tables 1(a) and 1(b) show the natural frequencies (ω), and modal damping (ζ) of the BWG antenna models, while Tables 2(a) and 2(b) show squared natural frequencies ($\Omega = \omega^2$), and damping ($d = 2\zeta\omega$). The latter are used later in the development of the uncertain model.

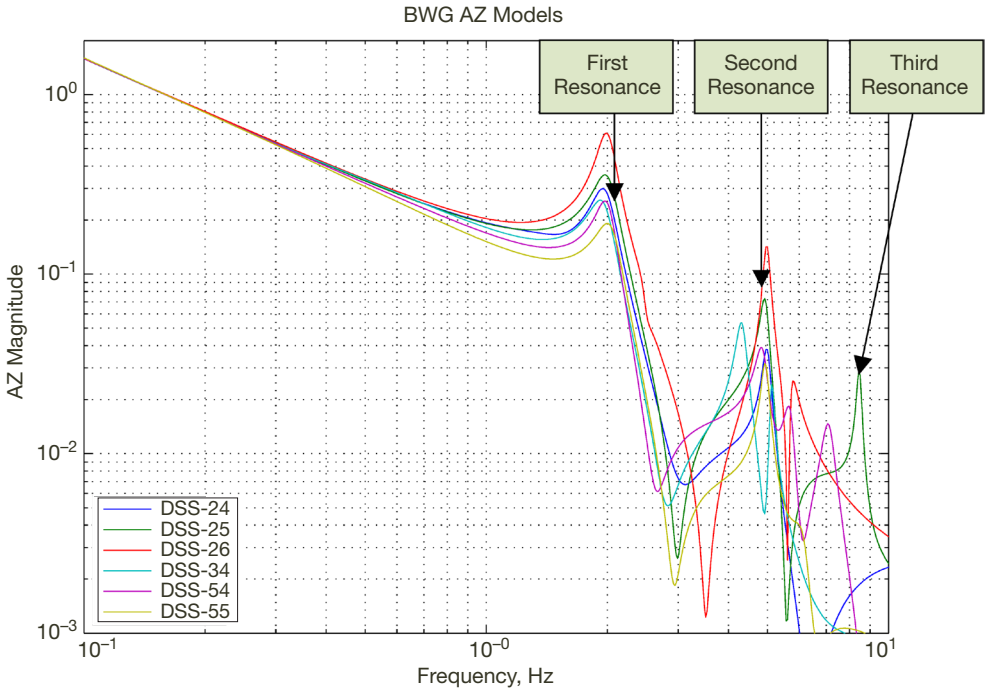

Figure 1. Magnitudes of the transfer functions of six BWG antennas.

III. Selection of the Nominal Model

One of the six antenna models is selected as a nominal model. This model is used to derive the H_∞ controller, and in the antenna servo coefficient file.

The selection process is as follows. The antenna stability and performance are impacted by the variations of the natural frequencies and damping. Thus, a model with natural frequencies and damping close to their mean values has small variations of the parameters. Any other model would produce larger variations. Tables 3(a) and 3(b) show the variations of natural frequencies and dampings from their mean, and Table 4 shows the rms values over

Table 1(a). Natural frequencies (ω), rad/s.

Antenna	First Mode	Second Mode
DSS-24	12.4134	31.3891
DSS-25	12.5774	31.0443
DSS-26	12.5652	31.3019
DSS-34	12.3048	32.1689
DSS-54	12.5874	30.5514
DSS-55	12.8273	31.0545
Mean	12.5459	31.2517

Table 1(b). Modal damping (ζ).

Antenna	First Mode	Second Mode
DSS-24	0.0701	0.0235
DSS-25	0.0702	0.0249
DSS-26	0.0536	0.0186
DSS-34	0.0722	0.0114
DSS-54	0.0577	0.0347
DSS-55	0.0726	0.0220
Mean	0.0661	0.0224

Table 2(a). Squared natural frequencies ($\Omega=\omega^2$).

Antenna	First Mode	Second Mode
DSS-24	154.0925	985.2756
DSS-25	158.1910	963.7486
DSS-26	157.8843	979.8089
DSS-34	151.4081	1034.8381
DSS-54	158.4426	933.3880
DSS-55	164.5396	964.3820
Mean	157.4263	976.9069

Table 2(b). Damping ($d= 2\zeta\omega$).

Antenna	First Mode	Second Mode
DSS-24	1.7412	1.4738
DSS-25	1.7650	1.5480
DSS-26	1.3472	1.1667
DSS-34	1.7759	0.7337
DSS-54	1.4520	2.1231
DSS-55	1.8635	1.3670
Mean	1.6575	1.4020

Table 3(a). Squared natural frequencies deviations from the mean.

Antenna	First Mode	Second Mode
DSS-24	–3.3338	8.3687
DSS-25	0.7647	–13.1583
DSS-26	0.4580	2.9020
DSS-34	–6.0182	57.9312
DSS-54	1.0163	–43.5189
DSS-55	7.1133	–12.5249

Table 3(b). Damping deviations from the mean.

Antenna	First Mode	Second Mode
DSS-24	0.0837	0.0718
DSS-25	0.1075	0.1460
DSS-26	–0.3102	–0.2354
DSS-34	0.1184	–0.6684
DSS-54	–0.2055	0.7210
DSS-55	0.2061	–0.0350

Table 4. rms of the natural frequency and damping deviations from the mean.

Antenna	RMS Value of Ω	RMS Value of *d*
DSS-24	9.0077	0.1103
DSS-25*	13.1804	0.1813
DSS-26	0.1813	0.3894
DSS-34	58.2434	0.6788
DSS-54	43.5309	0.7497
DSS-55	14.4037	0.2090

* DSS-25 selected as a nominal model.

the first two modes. The last table shows that the DSS-24, DSS-25, and DSS-26 antennas are the best candidates for the nominal model: their rms values are low. However, the DSS-26 antenna was eliminated as a nominal model candidate, since it has very low damping and large damping variations. Hence, its magnitude of the transfer function dominates other antenna responses (see Figure 1, red line). The remaining two antennas, on the other hand, have similar transfer functions, which are placed in the middle of the remaining transfer functions (cf. Figure 1). Thus, DSS-25 was selected as a nominal model.

IV. Uncertain Gains

Uncertain gains describe maximal deviations of the uncertain parameters. Denote, for simplicity of notation, Ω, as the square of natural frequency, i.e.,

$$\Omega = \omega^2 \tag{2}$$

and d as the damping coefficient defined as

$$d = 2\zeta\omega \tag{3}$$

Parameters Ω and d of the two first modes are the uncertain parameters of the antenna model.

A. Uncertain Gains of Natural Frequencies

With the above notation, the deviations (from the nominal) of the first and second natural frequencies are defined as

$$\begin{aligned} \alpha_{\Omega 1i} &= \frac{\Omega_{1i} - \Omega_{1nom}}{\Omega_{1nom}} \\ \alpha_{\Omega 2i} &= \frac{\Omega_{2i} - \Omega_{2nom}}{\Omega_{2nom}} \end{aligned} \tag{4}$$

The uncertain gains of the natural frequencies are the maximal absolute deviations of the natural frequencies from the nominal model. From Table 2(a), one obtains

$$\begin{aligned} \alpha_{\Omega 1} &= \tfrac{\max}{i}(|\alpha_{\Omega 1i}|) = 0.0428 \\ \alpha_{\Omega 2} &= \tfrac{\max}{i}(|\alpha_{\Omega 2i}|) = 0.0738 \end{aligned} \tag{5}$$

B. Uncertain Gains of Natural Damping

Similarly, the deviations (from the nominal) of the first and second natural damping are defined as

$$\begin{aligned} \alpha_{d1i} &= \frac{d_{1i} - d_{1nom}}{d_{1nom}} \\ \alpha_{d2i} &= \frac{d_{2i} - d_{2nom}}{d_{2nom}} \end{aligned} \tag{6}$$

The uncertain gains of the natural damping are the maximal absolute deviations of the natural damping from the nominal model. From Table 2(b), one obtains

$$\begin{aligned} \alpha_{d1} &= \tfrac{\max}{i}(|\alpha_{d1i}|) = 0.2367 \\ \alpha_{d2} &= \tfrac{\max}{i}(|\alpha_{d2i}|) = 0.5297 \end{aligned} \tag{7}$$

The coefficients $\alpha_{\Omega 1}, \alpha_{\Omega 2}, \alpha_{d1}, \alpha_{d2}$ are called the uncertain gains, and are used later in the uncertain model.

V. Antenna Uncertain Model

The uncertain model has its standard form, and is described in [7], pp. 20–23 and pp. 72–74, and [8], p. 57 and pp. 380–383.

A. Standard Uncertain Model

The uncertain model in this article describes all possible differences between the individual antennas, within the observed boundaries. In this way, a single model and single control coefficients can be used for all six antennas.

The uncertain model includes random parameters that span the variable properties of the antenna. These properties consist of the natural frequencies and damping of the first two flexible modes. Since the parameters spread randomly between the upper and lower bounds, the Monte Carlo analysis shall show the performance of almost all possible variations of antenna properties with a single set of servo coefficients.

In order to use it in the Matlab environment for the evaluation of the antenna performance, the uncertain model has to have a certain structure, as defined by the H_∞ controller design procedure (see [7], pp. 20–23 and pp. 72–74, and [8], p. 57 and pp. 380–383. This structure, called the standard uncertainty model, is shown in Figure 2. In this figure, G represents the nominal model and Δ is the parametric uncertain model that describes parameter variations. The uncertain block Δ is a diagonal matrix:

$$\Delta = \begin{bmatrix} \delta_1 & & 0 \\ & \ddots & \\ 0 & & \delta_n \end{bmatrix} \tag{8}$$

with the uncertain (random) parameters δ_i varying within the interval [–1, 1]

$$\delta_i \in [-1 \quad 1] \tag{9}$$

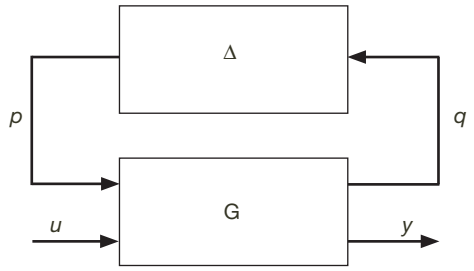

Figure 2. Standard configuration of an uncertain model: Δ is a matrix of random variables spanning the interval [–1 1].

Thus, the six BWG antennas are represented by a single (uncertain) model, shown above. In order to obtain this model, first an uncertain model for a single flexible mode is derived.

B. Uncertain Model Equations for a Single Mode

The equation of a single mode is as follows:

$$\begin{Bmatrix}\dot{x}_1\\ \dot{x}_2\end{Bmatrix}=\begin{bmatrix}0 & 1\\ -\Omega & -d\end{bmatrix}\begin{Bmatrix}x_1\\ x_2\end{Bmatrix}+\begin{bmatrix}0\\ b_u\end{bmatrix}u \tag{10}$$

The square of the uncertain natural frequency (Ω) is as follows:

$$\Omega=\Omega_{nom}(1+\alpha_\Omega\delta_\Omega) \tag{11}$$

and the uncertain damping coefficient (d) is as follows:

$$d=d_{nom}(1+\alpha_d\delta_d) \tag{12}$$

where Ω_{nom}, d_{nom} are nominal values of the natural frequency and damping, α_Ω, α_d are uncertain gains, and δ_Ω, δ_d are uncertain spreads, respectively, with

$$\begin{aligned}&\delta_\Omega\in[-1,\ \ 1]\\ &\delta_d\in[-1\ \ 1]\end{aligned} \tag{13}$$

In this way, the natural frequencies and damping vary between the maximal and minimal values, as measured for the BWG antennas.

Thus, the uncertain single-mode equation is as follows (the subscript *nom* is skipped for simplicity):

$$\begin{Bmatrix}\dot{x}_1\\ \dot{x}_2\end{Bmatrix}=\begin{bmatrix}0 & 1\\ -\Omega(1+\alpha_\Omega\delta_\Omega) & -d(1+\alpha_d\delta_d)\end{bmatrix}\begin{Bmatrix}x_1\\ x_2\end{Bmatrix}+\begin{bmatrix}0\\ b_u\end{bmatrix}u \tag{14}$$

Denoting

$$A=\begin{bmatrix}0 & 1\\ -\Omega & -d\end{bmatrix},\ \ B_u=\begin{bmatrix}0\\ b_u\end{bmatrix},\ \ x=\begin{Bmatrix}x_1\\ x_2\end{Bmatrix} \tag{15}$$

and

$$\begin{aligned}q_1&=-\Omega\alpha_\Omega x_1\\ q_2&=-d\alpha_d x_2\end{aligned} \tag{16}$$

one can rewrite Equation (14) as follows:

$$\dot{x}=Ax+B_u u+\begin{bmatrix}0 & 0\\ \delta_\Omega & \delta_d\end{bmatrix}\begin{Bmatrix}q_1\\ q_2\end{Bmatrix} \tag{17}$$

i.e.,

$$\dot{x}=Ax+B_u u+\begin{bmatrix}0 & 0\\ 1 & 1\end{bmatrix}\Delta\begin{Bmatrix}q_1\\ q_2\end{Bmatrix} \tag{18}$$

where

$$\Delta=\begin{bmatrix}\delta\Omega & 0\\ 0 & \delta_d\end{bmatrix},\ \ \delta_\Omega,\delta_d\in[-1\ \ 1] \tag{19}$$

In this way, Equation (18) is now

$$\dot{x} = Ax + B_u u + B_p \Delta q \tag{20}$$

where

$$B_p = \begin{bmatrix} 0 & 0 \\ 1 & 1 \end{bmatrix}, \quad \text{and} \quad q = \begin{Bmatrix} q_1 \\ q_2 \end{Bmatrix} \tag{21}$$

Note that p is the feedback, as in Figure 1:

$$p = \Delta q \tag{22}$$

where $p = \begin{Bmatrix} p_1 \\ p_2 \end{Bmatrix}$, therefore

$$\dot{x} = Ax + B_u u + B_p p \tag{23}$$

and

$$q = C_q x \tag{24}$$

where

$$C_q = \begin{bmatrix} -\Omega\alpha_\Omega & 0 \\ 0 & -d\alpha_d \end{bmatrix} \tag{25}$$

with the system output defined as follows

$$y = Cx, \quad C = \begin{bmatrix} 0 & 1 \end{bmatrix} \tag{26}$$

In summary, Equations (22–24) and (26) describe the uncertain mode model, and are collected as follows:

$$\begin{aligned} \dot{x} &= Ax + B_u u + B_p p \\ p &= \Delta q \\ q &= C_q x \\ y &= Cx \end{aligned}$$

where the matrices in the above equations are as follows:

$$\begin{aligned} A &= \begin{bmatrix} 0 & 1 \\ -\Omega & -d \end{bmatrix}, \quad \Delta = \begin{bmatrix} \delta_\Omega & 0 \\ 0 & \delta_d \end{bmatrix} \\ &\quad \delta_\Omega, \delta_d \in \begin{bmatrix} -1 & 1 \end{bmatrix} \\ B_u &= \begin{bmatrix} 0 \\ b_u \end{bmatrix}, \quad B = \begin{bmatrix} 0 \\ B_u \end{bmatrix}, \quad B_p = \begin{bmatrix} 0 & 0 \\ 1 & 1 \end{bmatrix} \\ C_q &= \begin{bmatrix} -\Omega\alpha_\Omega & 0 \\ 0 & -d\alpha_d \end{bmatrix}, \quad C = \begin{bmatrix} 0 & 1 \end{bmatrix} \end{aligned}$$

and the variables are

$$x = \begin{Bmatrix} x_1 \\ x_2 \end{Bmatrix}, \quad y = x_2$$
$$p = \begin{Bmatrix} p_1 \\ p_2 \end{Bmatrix}, \quad q = \begin{Bmatrix} q_1 \\ q_2 \end{Bmatrix}$$

C. Uncertain Model Equations for the Antenna

Based on the single-mode analysis, the antenna uncertain equations, with two uncertain modes, are as follows:

$$\begin{aligned} \dot{x} &= Ax + B_u u + B_p p \\ p &= \Delta q \\ q &= C_q x + D_q u \\ y &= C_y x \end{aligned} \tag{27}$$

where the state vector is

$$x = \begin{bmatrix} x_1 \\ x_2 \\ x_3 \\ x_4 \\ x_5 \end{bmatrix} \tag{28}$$

and the state matrices are as follows

$$A = \begin{bmatrix} \times & \times & \times & \times & \times \\ 0 & 0 & 1 & 0 & 0 \\ 0 & -\Omega_1 & -d_1 & 0 & 0 \\ 0 & 0 & 0 & 0 & 1 \\ 0 & 0 & 0 & -\Omega_2 & -d_2 \end{bmatrix} \tag{29}$$

$$B_u = \begin{bmatrix} \times \\ \times \\ \times \\ \times \\ \times \end{bmatrix}, \quad B_p = \begin{bmatrix} 1 & 0 & 0 & 0 & 0 \\ 0 & 0 & 0 & 0 & 0 \\ 0 & -\alpha_{\Omega 1} & -\alpha_{d1} & 0 & 0 \\ 0 & 0 & 0 & 0 & 0 \\ 0 & 0 & 0 & -\alpha_{\Omega 2} & -\alpha_{d2} \end{bmatrix} \tag{30}$$

(where $\times$ denotes a nonzero value of the nominal model), and

$$C_q = \begin{bmatrix} 0 & 0 & 0 & 0 & 0 \\ 0 & \Omega_1 & 0 & 0 & 0 \\ 0 & 0 & d_1 & 0 & 0 \\ 0 & 0 & 0 & \Omega_2 & 0 \\ 0 & 0 & 0 & 0 & d_2 \end{bmatrix}, \quad C_y = \begin{bmatrix} 1 & 0 & 0 & 0 & 0 \end{bmatrix} \tag{31}$$

$$D_q = \begin{bmatrix} \alpha_b \\ 0 \\ 0 \\ 0 \\ 0 \end{bmatrix} \tag{32}$$

while the uncertain inputs and outputs are

$$p = \begin{bmatrix} \delta_b u \\ \delta_{\Omega 1}\Omega_1 x_2 \\ \delta_{d1} d_1 x_3 \\ \delta_{\Omega 2}\Omega_2 x_4 \\ \delta_{d2} d_2 x_5 \end{bmatrix}, \quad q = \begin{bmatrix} u \\ \Omega_1 x_2 \\ d_1 x_3 \\ \Omega_2 x_4 \\ d_2 x_5 \end{bmatrix} \tag{33}$$

The uncertainty matrix is in the standard form

$$\Delta = \begin{bmatrix} \delta_b & 0 & 0 & 0 & 0 \\ 0 & \delta_{\Omega 1} & 0 & 0 & 0 \\ 0 & 0 & \delta_{d1} & 0 & 0 \\ 0 & 0 & 0 & \delta_{\Omega 2} & 0 \\ 0 & 0 & 0 & 0 & \delta_{d2} \end{bmatrix} \tag{34}$$

where

$$\delta_b, \delta_{\Omega 1}, \delta_{d1}, \delta_{\Omega 2}, \quad \text{and} \quad \delta_{d2} \in [-1 \;\; 1] \tag{35}$$

The closed-loop equation in an explicit form, for the system as in Figure 2, is as follows:

$$\begin{Bmatrix} \dot{x}_1 \\ \dot{x}_2 \\ \dot{x}_3 \\ \dot{x}_4 \\ \dot{x}_5 \end{Bmatrix} = \begin{bmatrix} \times & \times & \times & \times & \times \\ 0 & 0 & 1 & 0 & 0 \\ 0 & -\Omega_1(1+\delta_{\Omega 1}\alpha_{\Omega 1}) & -d_1(1+\delta_{d1}\alpha_{d1}) & 0 & 0 \\ 0 & 0 & 0 & 0 & 1 \\ 0 & 0 & 0 & -\Omega_2(1+\delta_{\Omega 2}\alpha_{\Omega 2}) & -d_2(1+\delta_{d2}\alpha_{d2}) \end{bmatrix} \begin{Bmatrix} x_1 \\ x_2 \\ x_3 \\ x_4 \\ x_5 \end{Bmatrix}$$
$$+ B_u u + \begin{bmatrix} \delta_b \alpha_b \\ 0 \\ 0 \\ 0 \\ 0 \end{bmatrix} u \tag{36}$$

where for the azimuth model

$$\alpha_{\Omega 1} = 0.0428, \quad \alpha_{\Omega 2} = 0.0738, \quad \alpha_{d1} = 0.4227, \quad \alpha_{d2} - 0.5297$$

One sees that the natural frequencies vary up to 7 percent, while damping up to 53 percent.

Combining Equation (27) gives

$$\begin{aligned} \dot{x} &= (A + B_p \Delta C_q)x + (B_u + B_p \Delta D_q)u \\ y &= C_y x \end{aligned} \tag{37}$$

The above system is in a standard robust representation [7], and is illustrated as in Figure 3, which is a detail representation of the standard form from Figure 2.

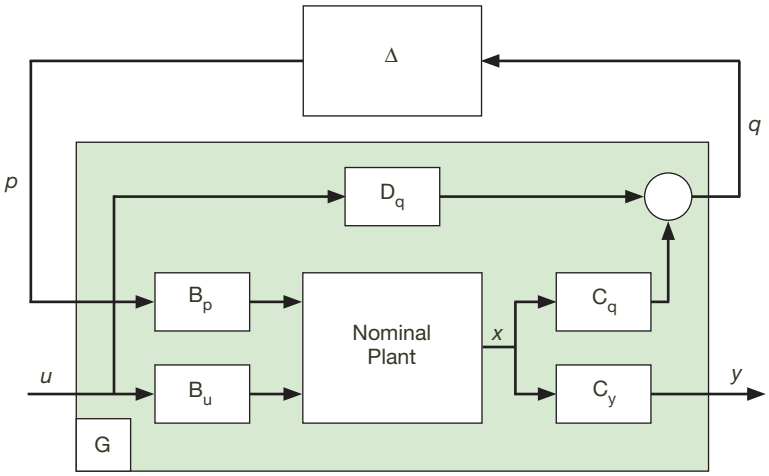

Figure 3. Block diagram of the antenna uncertain model.

D. Upper and Lower Bounds of the Nominal Model

For the above equations, the Matlab code generated the nominal, and upper and lower bounds, of the transfer function of the uncertain model, which are shown in Figure 4.

This model will be used in the development of the robust controller for the BWG antennas.

VI. The H_∞ Controller Design

A typical approach to the robust design of the H_∞ controller is to use the μ synthesis procedure with D-K iterations; see, for example, [7]. However, the μ synthesis was tried, and did

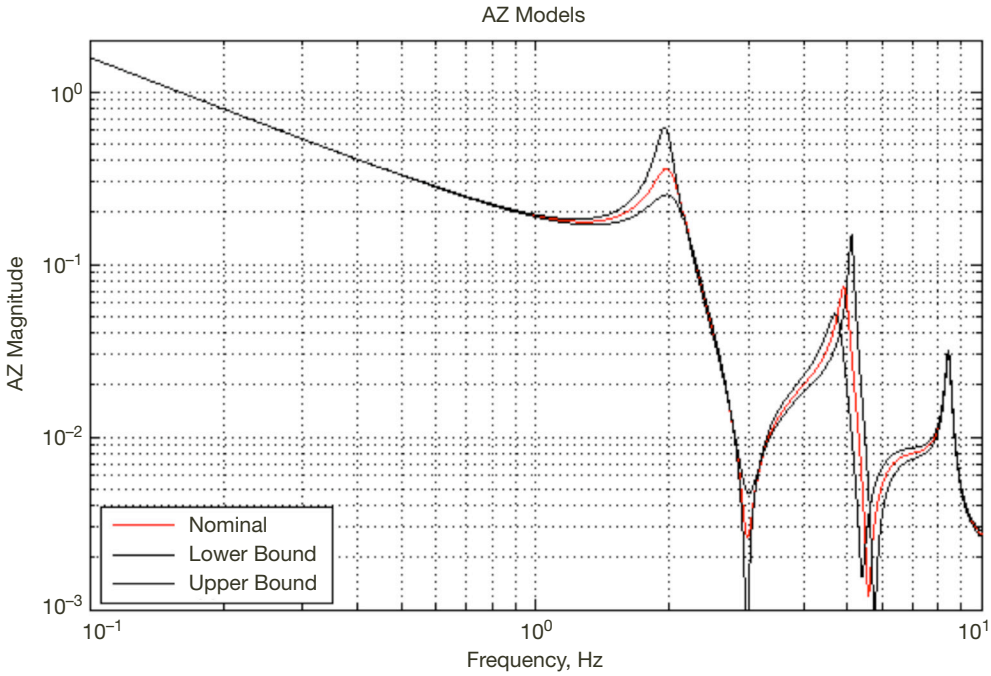

Figure 4. Upper and lower bounds of the magnitude of the transfer function of the uncertain model.

not work successfully for the BWG antenna model. It did not converge successfully. As it was also observed in [7] (p. 222), "the uncertainties of resonant modes would make the D-K iterations difficult to converge. This confirms that the resonant modes may create difficulties in the controller design." Thus, for the antenna purposes instead of μ synthesis, the H_∞ design method presented in [9] was used, and the uncertainty of the antenna model was tested using the Monte Carlo iterations.

A. Short Description of the Design Process

The design process for the H_∞ controller is described in [9]. The block diagram for the H_∞ controller is presented in Figure 5. The closed-loop equations are presented for the controller as in Figure 5. From this figure, they are as follows:

$$\begin{aligned} \dot{x}_{cl} &= A_{cl}x_{cl} + B_{cl}r + B_w w \\ y &= C_{cl}x_{cl} + D_{21}w \\ z &= C_1 x + D_{21}u \end{aligned} \tag{38}$$

where the closed-loop state (x_{cl}) consists of the integral of the antenna position (e_i), the antenna state (x), and the estimator state $(\hat{x})$, i.e.,

$$x_{cl} = \begin{Bmatrix} e_i \\ x \\ \hat{x} \end{Bmatrix} \tag{39}$$

The corresponding closed-loop state matrices are as follows:

$$A_{cl} = \begin{bmatrix} 0 & 0 & -C_2 \\ B_2 k_i & A & -B_2 k_p C_2 - B_2 k_f C_1 \\ B_2 k_i & k_e C_2 & A - k_e C_2 - B_2 k_p C_2 - B_2 k_f C_1 + \rho^{-2} B_1 B_1^T S_{\infty c} \end{bmatrix} \tag{40}$$

$$B_{cl} = \begin{bmatrix} 1 \\ B_2 k_p \\ B_2 k_p \end{bmatrix}, \quad B_w = \begin{bmatrix} 0 \\ B_1 \\ 0 \end{bmatrix}, \quad C_{cl}\begin{bmatrix} 0 & C_p & 0 \end{bmatrix} \tag{41}$$

The matrix K_c is the controller gain, while K_e is the estimator gain. The controller gain is obtained as follows:

$$K_c = B_2^T S_{\infty c} \tag{42}$$

while the estimator gain is given as

$$\begin{aligned} K_e &= S_o S_{\infty e} C_2^T \\ S_o &= (I - \rho^{-2} S_{\infty e} S_{\infty c})^{-1} \end{aligned} \tag{43}$$

The matrices $S_{\infty c}$ and $S_{\infty e}$ in the gain equations are obtained from the Riccati equations, namely:

$S_{\infty c}$ is the solution of the H_∞ controller Riccati equation (HCARE)

$$S_{\infty c}A + A^T S_{\infty c} + C_1^T C_1 - S_{\infty c}(B_2 B_2^T - \rho^{-2} B_1 B_1^T) S_{\infty c} = 0 \tag{44}$$

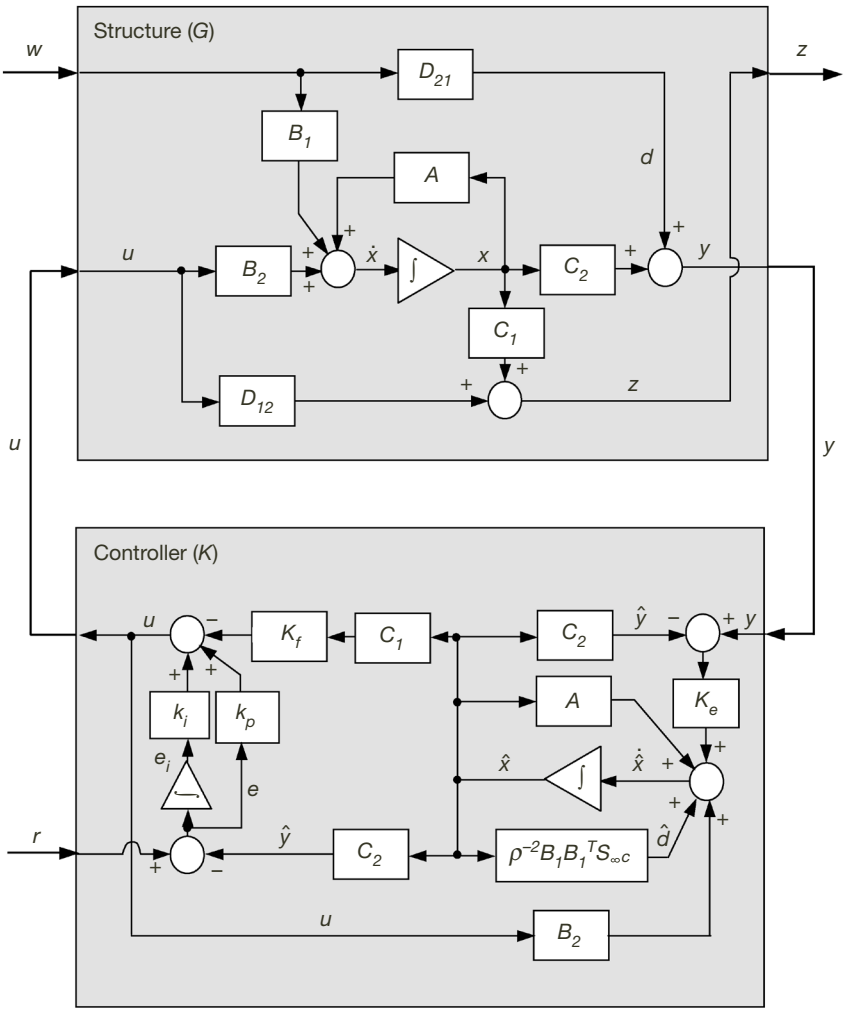

Figure 5. An H_∞ controller structure.

$S_{\infty e}$ is the solution of the H_∞ estimator Riccati equation (HFARE)

$$S_{\infty e}A^T + AS_{\infty e} + B_1B_1^T - S_{\infty e}(C_2^TC_2 - \rho^{-2}C_1^TC_1)S_{\infty e} = 0 \tag{45}$$

and the above solutions must satisfy the following inequality:

$$\lambda_{\max}(S_{\infty c}S_{\infty e}) < \rho^2 \tag{46}$$

where $\lambda_{\max}(S_{\infty c}S_{\infty e})$ is the largest eigenvalue of $S_{\infty c}S_{\infty e}$, and ρ is the parameter in Equations (44) and (45).

B. Simulation of the H_∞ Controller Performance

Using the DSS-25 antenna (azimuth) model and the above approach, the H_∞ controller has been derived. Its performance is described by

(1) The step response, shown in Figure 6. From the step response, the settling time is 4.9 s, and overshoot is 16 percent.

(2) The magnitude of the closed-loop transfer function is shown in Figure 7. From this plot, the bandwidth is 0.43 Hz.

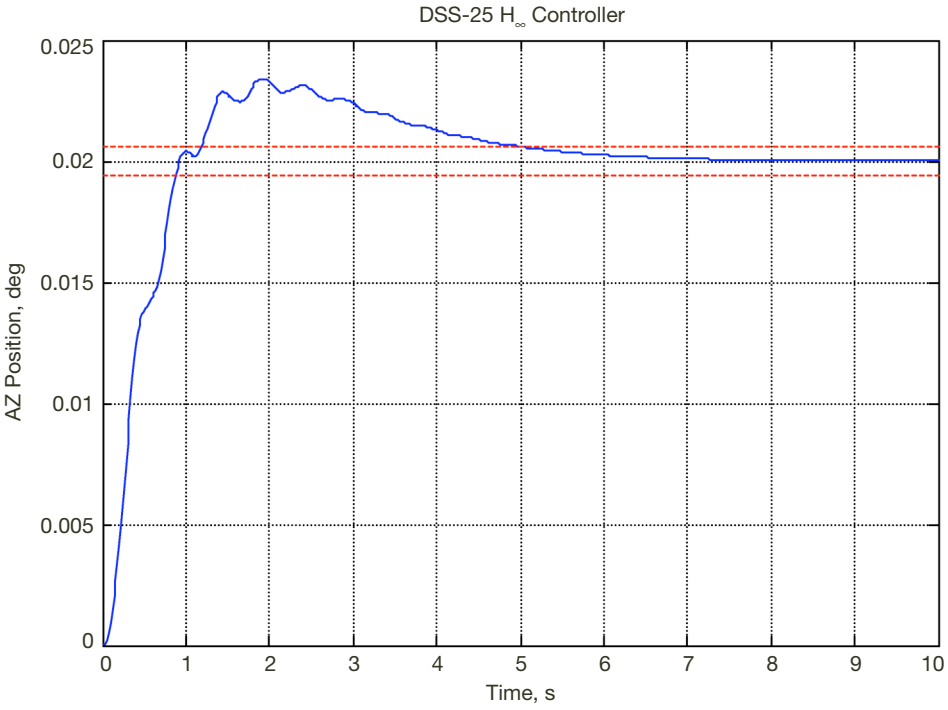

Figure 6. Step response of the DSS-25 H_∞ controller: settling time 4.9 s, overshoot 16 percent.

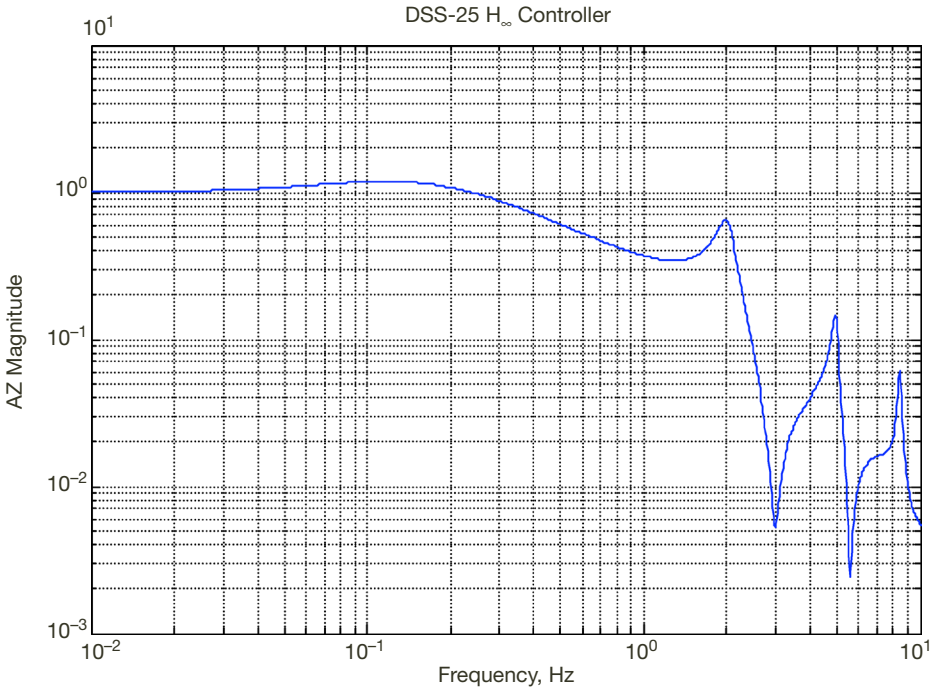

Figure 7. Magnitude of the DSS-25 closed-loop transfer function (bandwidth = 0.43 Hz).

(3) The servo error in 20 mph wind gusts was simulated, and the result is shown in Figure 8. The plot shows the rms servo error of 0.17 mdeg.

The performance is summarized in Table 5, and is compared with the existing LQG controllers in Table 6. One can see that the H_∞ controller performance is similar or exceeds the LQG controller performance (except for the DSS-25 antenna, which LQG controller was designed exceptionally strong).

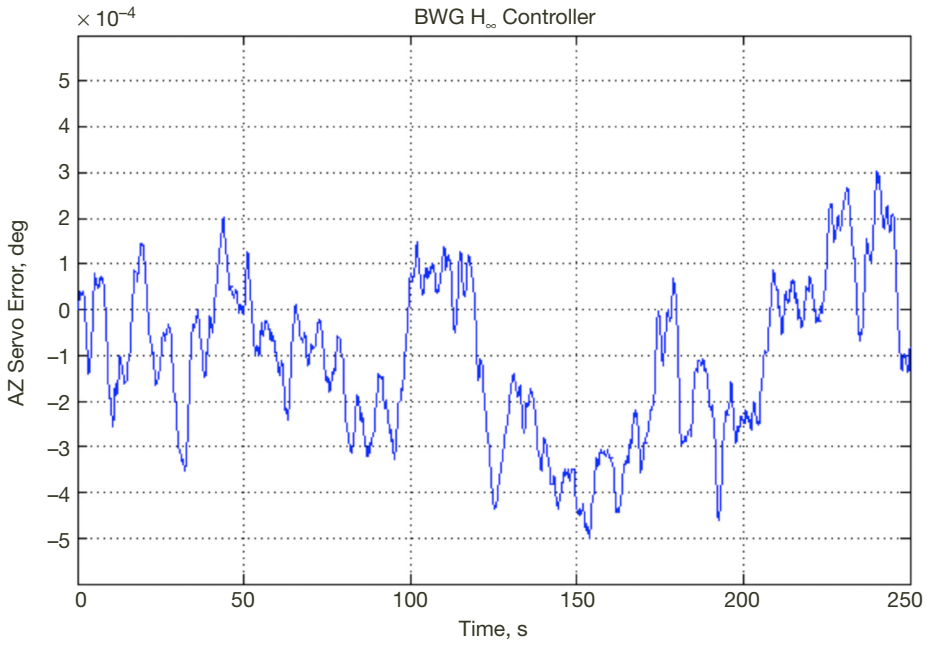

Figure 8. Servo error in 20-mph wind gusts.

Table 5. Performance of the H_∞ controller.

Performance Parameter	Performance
Settling time	4.9 s
Overshoot	16 percent
Bandwidth	0.43 Hz
rms servo error	0.17 mdeg

Table 6. A comparison of the performance of the current LQG controllers and the H_∞ controller.

Antenna	Settling time, s	Overshoot, percent
DSS-24	8.2	16
DSS-25	3.8	15
DSS-26	7.5	18
DSS-34	5.1	17
DSS-54	8.0	20
DSS-55	5.9	16
H_∞	4.9	16

VII. Closed-Loop Performance Evaluation Using Monte Carlo Simulations

The block diagram of the closed-loop system with the parameter variations Δ that span the variable parameter range of all BWG antennas is shown in Figure 9. The performance of the BWG antennas is simulated using the H_∞ controller obtained for the DSS-25 antenna, and varying randomly the gains in matrix Δ that represent the antenna model uncertainty. Over 10,000 Monte Carlo simulations have been performed to evaluate the performance over the parameter variation span.

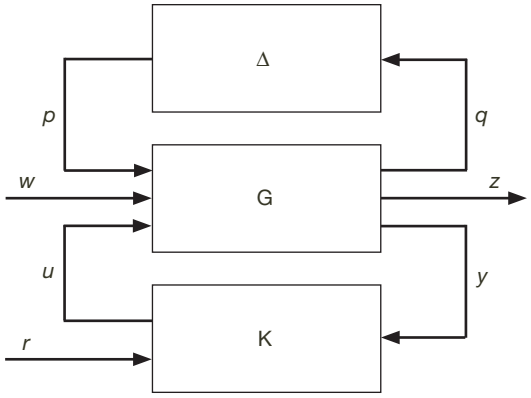

Figure 9. The H_∞ closed-loop system with uncertain antenna model: G – nominal plant, K – H_∞ controller, Δ – matrix of random variables that model the antenna uncertainty, *μ* – velocity input, *w* – disturbances, *y* – encoder, and z – servo error.

Before reviewing the results, the open-loop transfer function with all modeled uncertainties is shown in Figure 10 (10,000 deviations for each frequency).

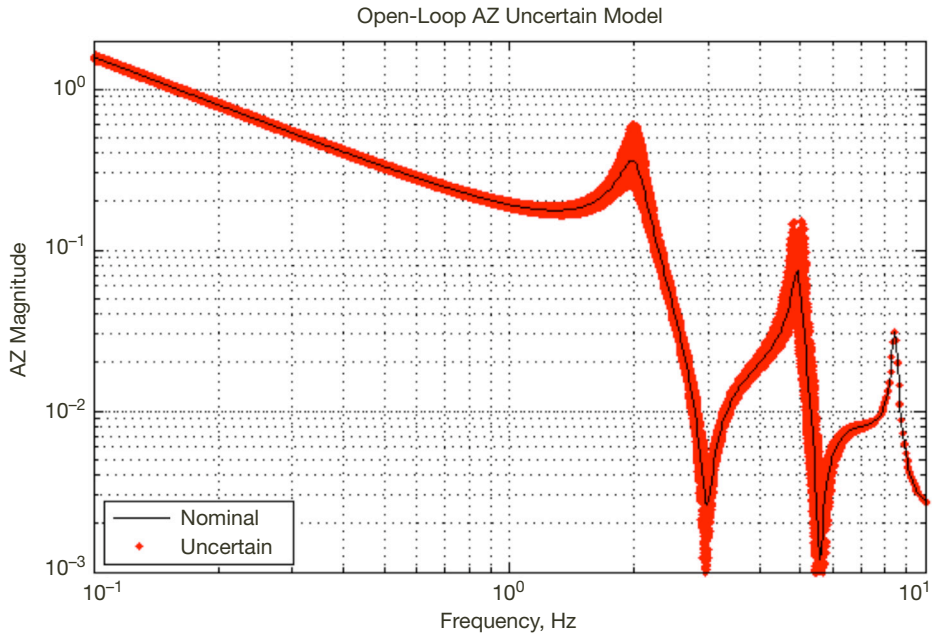

Figure 10. Open-loop magnitude of transfer function with uncertain deviations: black line – nominal model, red dots – model variations (10,000 for each frequency).

Next, the closed-loop performance using the Monte Carlo approach was simulated. The results are shown in Figures 11(a)–(d). One can see that the system is stable for all allowable deviations of antenna parameters. The resulting deviations in the step responses, Figure 11(a), from the nominal model are small, as well as the deviations in the disturbance step responses, Figure 11(b), magnitudes of the transfer function, Figure 11(c), and magnitudes of the disturbance transfer functions, Figure 11(d). Thus, the controller performance should satisfy the requirements at all BWG antennas.

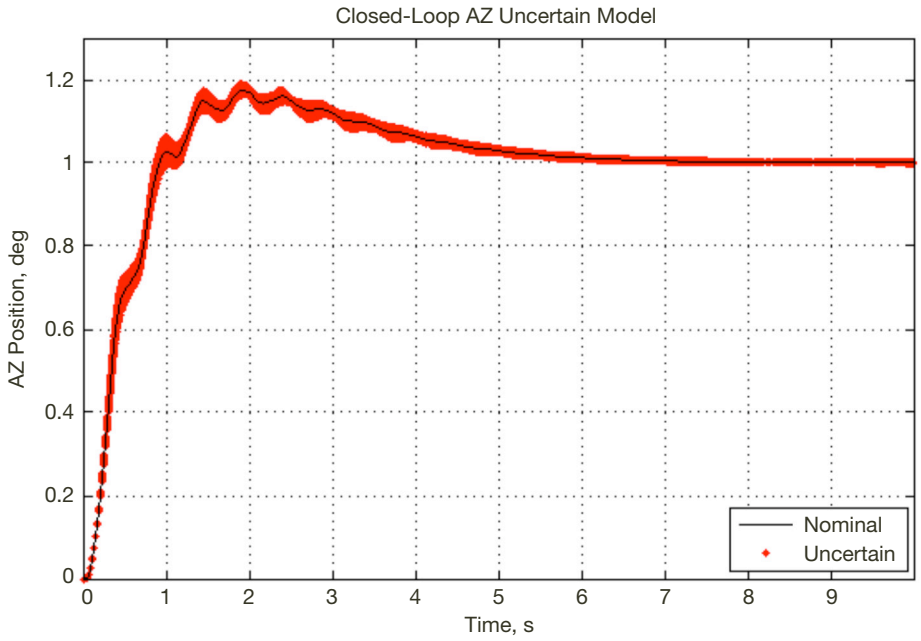

Figure 11(a). Closed-loop step response with uncertain deviations: black line – nominal model, red dots – model variations (10,000 for each time instant).

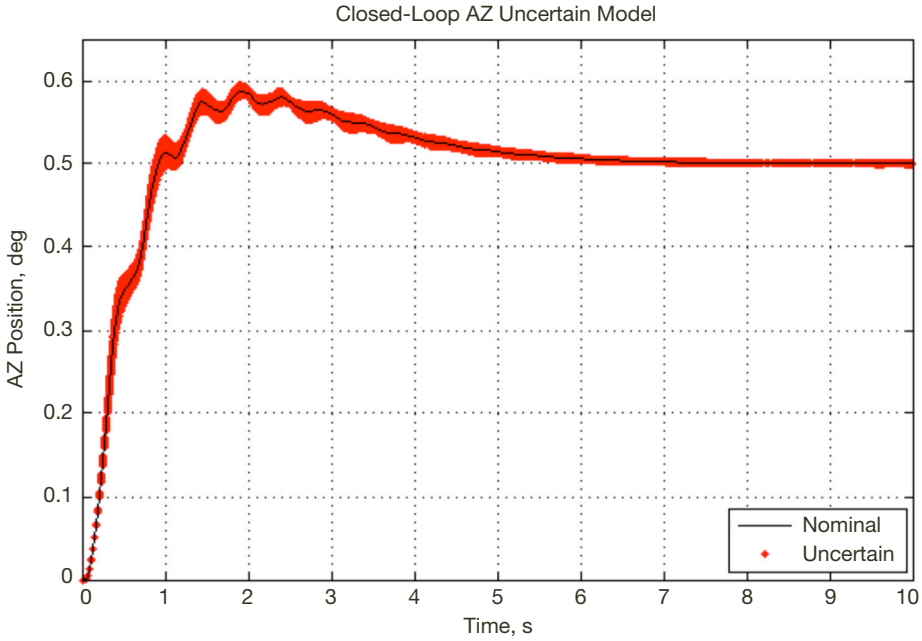

Figure 11(b). Closed-loop disturbance step response with uncertain deviations: black line – nominal model, red dots – model variations (10,000 for each time instant).

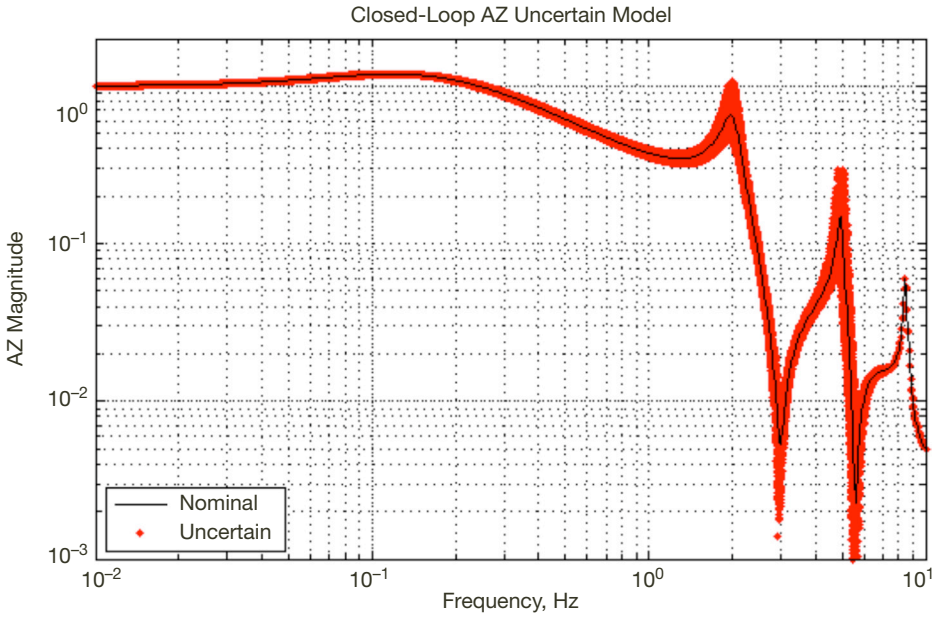

Figure 11(c). Closed-loop magnitude of transfer function with uncertain deviations: black line – nominal model, red dots – model variations (10,000 for each frequency).

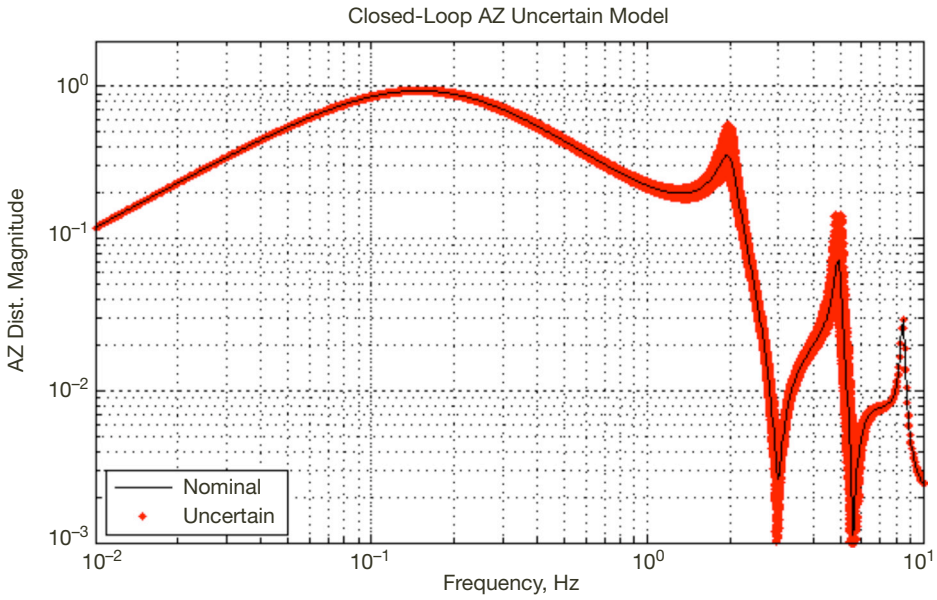

Figure 11(d). Closed-loop magnitude of disturbance transfer function with uncertain deviations: black line – nominal model, red dots – model variations (10,000 for each frequency).

In order to check it, the H_∞ controller from the DSS-25 antenna was applied to all six antennas. The results are shown in Figures 12(a)–(d). The plots show that the antennas are stable, and their performance is close to the nominal model performance that satisfies the requirements.

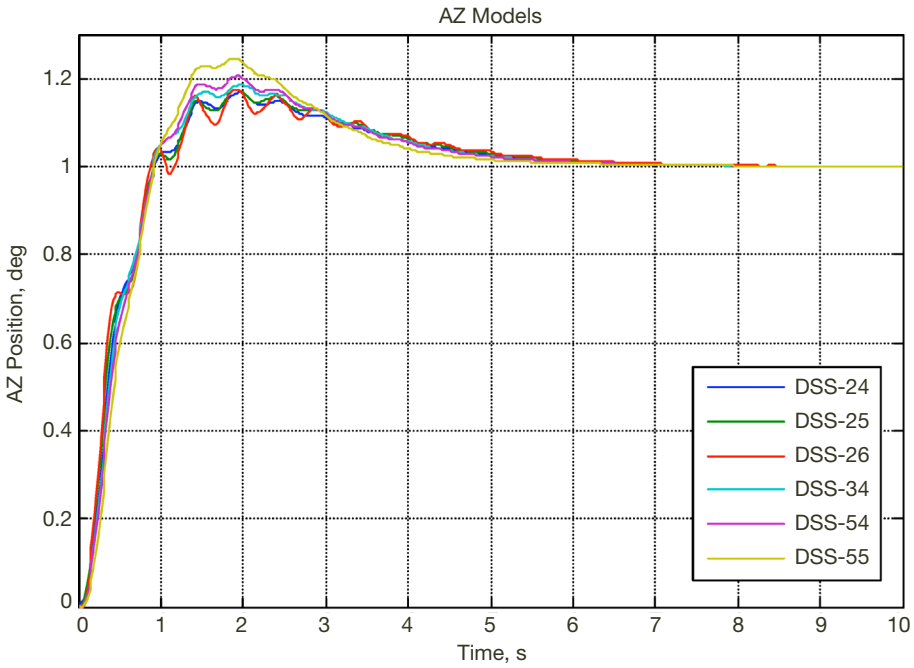

Figure 12(a). The H_∞ closed-loop step responses of the BWG antennas.

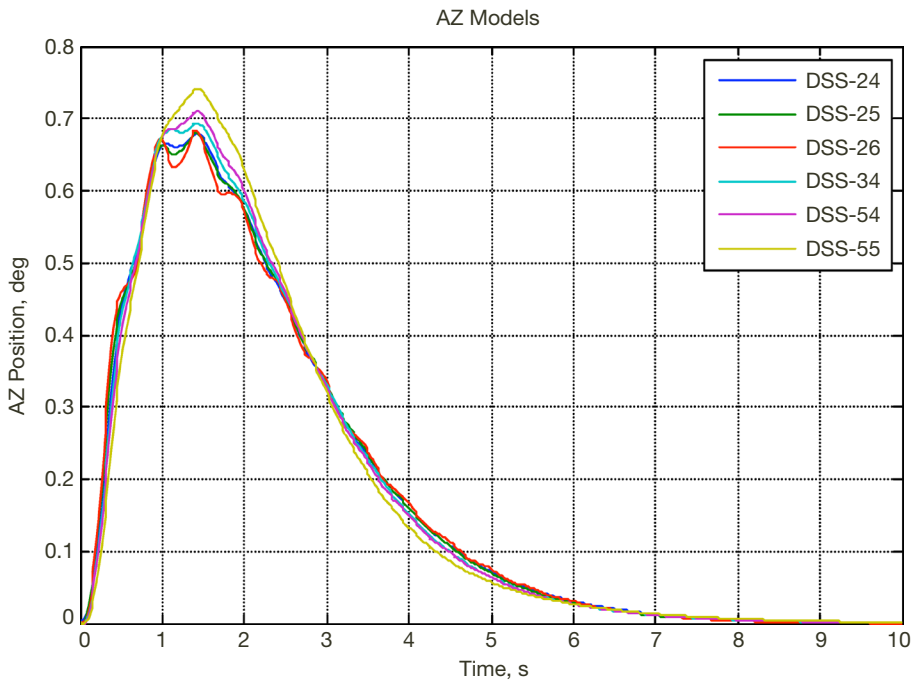

Figure 12(b). The H_∞ closed-loop disturbance step responses of the BWG antennas.

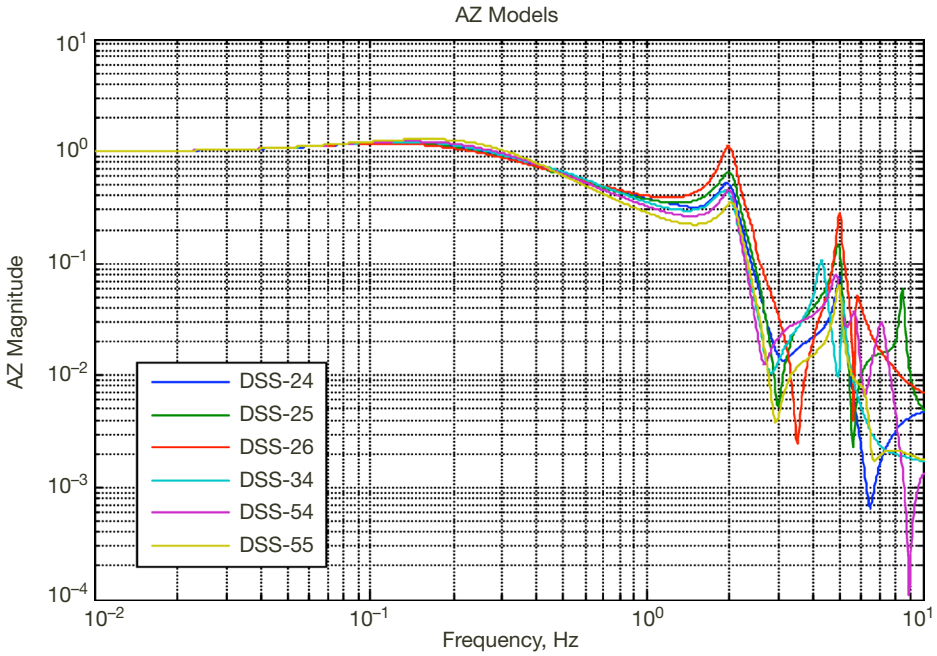

Figure 12(c). Magnitudes of the H_∞ closed-loop transfer function of the BWG antennas.

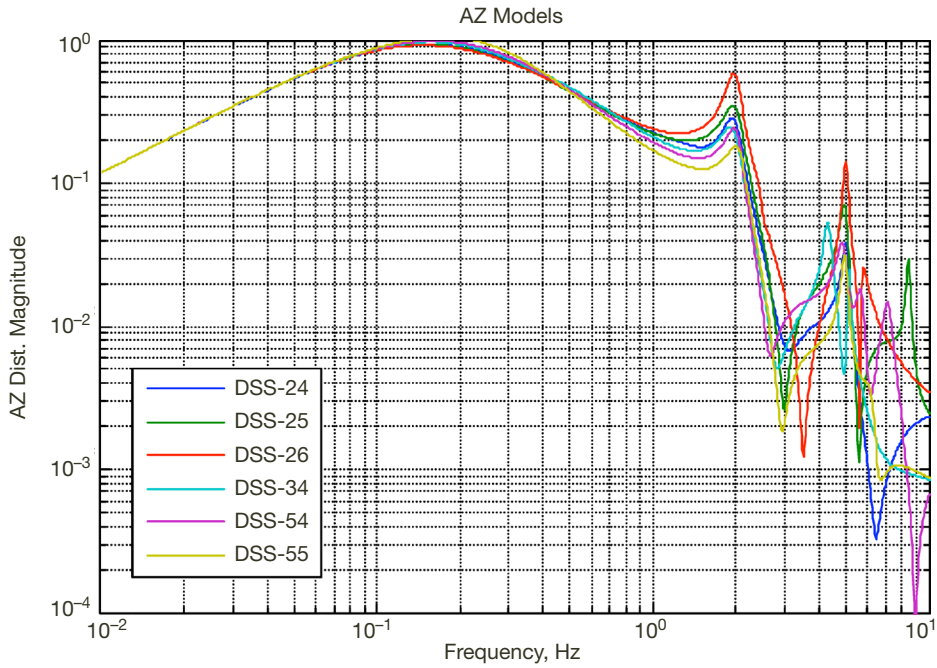

Figure 12(d). Magnitudes of the H_∞ closed-loop disturbance transfer function of the BWG antennas.

VIII. Conclusions

The analysis and the results of over 10,000 Monte Carlo simulations showed that a single set of the H_∞ controller could be used for all BWG antennas. The H_∞ controller performance is similar or exceeds the existing LQG controllers, except for the DSS-25 antenna controller. Note that the latter controller was derived exceptionally strong and is stable at the DSS-25 antenna. At the remaining antennas, the controller coefficients are weaker, and represent the "standard" LQG performance.

References

[1] T. Erm, B. Bauvir, and Z. Hurak, "Time to Go H-infinity?" *Proceedings of SPIE, Advanced Software, Control, and Communication Systems for Astronomy*, Glasgow, UK, vol. 5496, 2004.

[2] W. Gawronski, "H_∞ controller for the DSS-13 Antenna with Wind Disturbance Rejection Properties," *The Telecommunications and Data Acquisition Progress Report*, vol. 42-127, Jet Propulsion Laboratory, Pasadena, California, pp. 1–15, July–September 1996, published November 15, 1996.
http://ipnpr.jpl.nasa.gov/progress_report/42-127/127G.pdf

[3] W. Gawronski, "Antenna Control Systems: From PI to H_∞," *IEEE Antennas and Propagation Magazine*, vol. 43, no. 1, pp. 52–60, February 2001.

[4] K. Li, E. B. Kosmatopoulos, P. A. Ioannou, and H. Ryaciotaki-Boussalis, "Large Segmented Telescopes: Centralized, Decentralized, and Overlapping Control Designs," *IEEE Control Systems Magazine*, vol. 20, no. 5, pp. 59–72, 2000.

[5] J. N. Juang, *Applied System Identification*, Englewood Cliffs: Prentice Hall, 1994.

[6] L. Ljung, *System Identification*, Englewood Cliffs: Prentice Hall, 1987.

[7] D. W. Gu, P. H. Petkov, and M. M. Konstantinov, *Robust Control Design with Matlab*, London: Springer, 2005.

[8] U. Mackenroth, *Robust Control Systems*, Berlin: Springer, 2004.

[9] W. Gawronski, *Modeling and Control of Antennas and Telescopes*, New York: Springer, 2008.